Resonance in Formamide and Its Chalcogen Replacement Analogues: A Natural Population Analysis/Natural Resonance Theory Viewpoint

Eric D. Glendening* and John A. Hrabal II

Contribution from the Department of Chemistry, Indiana State University, Terre Haute, Indiana 47809

Received January 9, 1997. Revised Manuscript Received October 14, 1997[⊗]

Abstract: The influence of resonance on the structure and rotation barrier of formamide and its S, Se, and Te replacements analogues is examined using the natural bond orbital methods. Calculations are performed at the RHF, B3LYP, and MP2 levels of theory with 6-31+G* basis sets and effective core potentials. At the MP2 level, the rotation barriers increase with the increasing size of the chalcogen, from 17.2 kcal mol^{-1} for formamide to 21.0 kcal mol^{-1} for telluroformamide. Natural population analysis and natural resonance theory (NRT) reveal shifts in the charge density that are consistent with the strong resonance stabilization of the equilibrium, planar geometries. NRT provides a simple, quantitative description of the amides as a resonance hybrid consisting primarily of two contributing structures, the parent Lewis structure and a secondary dipolar form. Amide resonance effects strengthen from formamide to telluroformamide as the weight of the dipolar form increases. Polarizability appears to contribute importantly, allowing the chalcogens to accommodate more charge density than anticipated on the basis of electronegativity.

I. Introduction

Amide structure and reactivity is conventionally interpreted within the framework of resonance theory.[1,2] Formamide, the simplest amide, is poorly represented by the single Lewis structure **I** (X = O). Its planar geometry, large rotation barrier (18−19 kcal mol^{-1}), and red-shifted carbonyl stretching frequency can be readily understood in terms of the strong resonance mixing of the dipolar form **II**. In contrast to typical

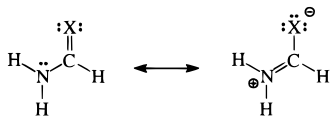

I **II**

pyramidal amine geometries, the planar amino group is stabilized by the resonance interaction of the p-type N lone pair with the carbonyl π system. The resulting CN double-bond character gives rise to the large rotation barrier, while the loss of CO double-bond character leads to a low CO stretching frequency. Amide resonance has been extensively discussed for decades and is now firmly embedded in standard textbooks of organic chemistry.[3]

The traditional amide resonance model has, however, been challenged in recent years, primarily by Wiberg, Laidig, and co-workers.[4−11] Their criticisms largely stem from computational studies of formamide in its planar (**1a**) and twisted (**2a**)

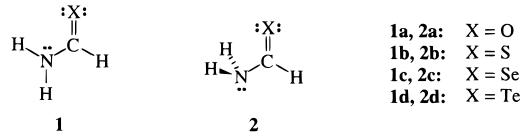

1a, 2a: X = O
1b, 2b: X = S
1c, 2c: X = Se
1d, 2d: X = Te

1 **2**

geometries. The twisted geometry should be only weakly stabilized by resonance interactions as the N lone pair lies in the σ frame, antiperiplanar to the σ_{CO} bond. Resonance theory suggests that the charge density of **1a** should reflect, through the contribution of **II**, a transfer of (negative) charge from N to O relative to that of **2a**. An analysis of calculated charge densities using Bader's atoms in molecules (AIM) method[12] reveals, however, the transfer of charge from C to N with minimal change in the charge at O. Amide resonance further predicts the elongation of the CN bond and contraction of the CO bond as the planar geometry rotates into the twisted form, **1a** → **2a**. While these bond length changes are indeed observed in the calculations, the CN elongation (∼0.08 Å) is considerably more pronounced than the CO contraction (∼0.01 Å). Thus, it appears that the CN bond gains significant double-bond character, whereas the CO remains essentially a double bond. The resonance model might lead one to expect more similar changes in bond length on rotation.

Thioformamide (**1b**) also presents an apparent difficulty for the traditional resonance model.[9,10] A weaker contribution from the dipolar structure **II** (X = S) and, hence, lower rotation barrier are anticipated on the basis of the relative electronegativities of O and S. However, *ab initio* calculations suggest that

* Corresponding author. E-mail: ericg@chem.indstate.edu.

[⊗] Abstract published in *Advance ACS Abstracts,* December 15, 1997.

(1) Pauling, L. *The Nature of the Chemical Bond,* 3rd ed.; Cornell University: Ithaca, NY, 1960.
(2) Wheland, G. W. *Resonance in Organic Chemistry*; Wiley: New York, 1955.
(3) See, e.g.: (a) Carey, F. A. *Organic Chemistry,* 3rd ed.; McGraw-Hill: New York, 1996; p 809. (b) McMurry, J. *Organic Chemistry,* 4th ed.; Brooks/Cole: New York, 1996; p 942. (c) Solomons, T. W. G. *Organic Chemistry,* 6th ed.; Wiley: New York, 1996; p 906.
(4) Wiberg, K. B.; Laidig, K. E. *J. Am. Chem. Soc.* **1987**, *109,* 5935.
(5) Wiberg, K. B.; Breneman, C. M. *J. Am. Chem. Soc.* **1992**, *114,* 831.
(6) Wiberg, K. B.; Hadad, C. M.; Rablen, P. R.; Cioslowski, J. *J. Am. Chem. Soc.* **1992**, *114,* 8644.
(7) Wiberg, K. B.; Rablen, P. R. *J. Am. Chem. Soc.* **1993**, *115,* 9234.
(8) Laidig, K. E.; Cameron, L. M. *Can. J. Chem.* **1993**, *71,* 872.
(9) Wiberg, K. B.; Rablen, P. R. *J. Am. Chem. Soc.* **1995**, *117,* 2201.
(10) Laidig, K. E.; Cameron, L. M. *J. Am. Chem. Soc.* **1996**, *118,* 1737.
(11) Also see: Knight, E. T.; Allen, L. C. *J. Am. Chem. Soc.* **1995**, *117,* 4401.
(12) Bader, R. F. W. *Atoms in Molecules: A Quantum Theory*; Clarendon Press: Oxford, U.K., 1990.

S0002-7863(97)00074-7 CCC: $14.00

thioformamide has, in fact, a larger barrier than formamide. Furthermore, AIM again reveals the significant transfer of charge from C to N in the planar geometry (rather than from N to S). Laidig and Cameron[10] thus argued that resonance is relatively unimportant in thioformamide. Wiberg and Rablen,[9] however, found significant transfer of π density from N to S in electron density difference maps. They concluded that the amide resonance picture is more appropriate for describing the thioamides than their O-based analogues.

In the present work, we reexamine the role of resonance interactions in formamide, thioformamide, and their Se and Te replacement analogues. Whereas previous studies[4−10] focused largely on the AIM analysis of the calculated charge densities, we present here an alternative analysis of amide resonance based on Weinhold's natural bond orbital (NBO) methods.[13−16] In contrast to the AIM results, NBO provides a simple, quantitative description of the amides that is consistent with the conventional resonance-based picture. Particular attention is focused on the natural population analysis (NPA)[14] and natural resonance theory (NRT)[15] treatment of the calculated charge densities.

II. Methods

Electronic structure calculations were carried out using the Gaussian 94[17] and GAMESS[18] programs. Geometries were fully optimized at the RHF, MP2, and B3LYP levels of theory.[19,20] Standard 6-31+G* basis sets were employed for H, C, N, O, and S together with the effective core potentials (ECPs) and valence basis sets for Se and Te of Bergner *et al.*[21] The latter are [2s3p] contractions of (4s5p) primitive sets, augmented by standard d-type polarization functions [α_d(Se) = 0.315, α_d(Te) = 0.237][18] and by diffuse s- and p-type functions [α_s(Se) = 0.050224, α_p(Se) = 0.010550, α_s(Te) = 0.041359, α_p(Te) = 0.009158].

Resonance effects in the amides were investigated using NRT,[15] which describes calculated charge densities in terms of resonance structures, weights, and bond orders. Briefly, the NRT formalism expands the one-electron, reduced density operator $\hat{\Gamma}$,

$$\hat{\Gamma} = N\int \Psi(1,2,...,N)\,\Psi^*(1',2,...,N)\,d2...dN \qquad (1)$$

as a ''resonance hybrid'' of density operators $\{\hat{\Gamma}_\alpha\}$,

$$\hat{\Gamma} \approx \sum_\alpha w_\alpha \hat{\Gamma}_\alpha \qquad (2)$$

where each $\hat{\Gamma}_\alpha$ corresponds to the idealized resonance structure wavefunction Ψ_α. The resonance weights $\{w_\alpha\}$ are variationally optimized to give the best description of $\hat{\Gamma}$, subject to the constraints

$$w_\alpha \geq 0, \quad \sum_\alpha w_\alpha b_{AB}^{(\alpha)} \qquad (3)$$

The natural bond order between any two atoms A and B is given by the expression

$$b_{AB} = \sum_\alpha w_\alpha b_{AB}^{(\alpha)} \qquad (4)$$

where $b_{AB}^{(\alpha)}$ is the integer number of bonds between the two atoms in resonance structure α.

For closed-shell calculations, the density operators $\{\hat{\Gamma}_\alpha\}$ of eq 2 are constructed from doubly occupied NBOs.[13] Covalent-ionic resonance interactions of, for example, the form **A** ↔ **B**

A **B**

are treated by single ''polar covalent'' structures (of connectivity **A**) comprised of polarized NBOs. By permitting ionic character to enter the resonance hybrid through the polar covalence of the contributing structures, NRT avoids rather lengthy expansions and instead describes the molecular charge density using only a handful of structures. NRT typically generated ∼15−20 candidate structures for the amides studied here, but only a few of these retained any significant weight following optimization. Due to the rather strong delocalizing interactions in the planar amides, a two-reference NRT treatment (based on both structures **I** and **II**) was performed for all geometries. Additional details of the NRT implementation are provided elsewhere.[15,16]

III. Geometries and Rotation Barriers

Three stationary points were calculated for each of the amides. These correspond to the planar equilibrium geometries **1** and the two ''twisted'' saddle point geometries **2** and **3**. The latter,

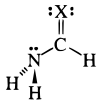

3

with the N lone pair antiperiplanar to the CH bond, are somewhat less stable than the geometries of **2** (by 2.4, 1.6, 1.7, and 1.1 kcal mol^{-1} for X = O, S, Se, and Te, respectively, at the MP2 level). The optimized CX and CN bond lengths for **1** and **2** are listed in Table 1, together with the calculated rotation barriers. We also optimized at each level of theory several additional geometries along the **1** → **2** torsional profile. A ghost center was attached to C such that it makes constrained dihedral angles of $\pm\phi$ with the two amino H atoms. In the planar geometry **1** (the 0° rotamer), the C-ghost line of centers is normal to the plane of the molecule. Rotation of the ghost about C in 15° increments with full reoptimization of the angle ϕ and all other internal coordinates gave a series of five intermediate rotamers along the minimum energy path up to the saddle point **2** (the 90° rotamer). Figure 1 shows the resulting torsional profiles for the amides at the MP2 level.

Chalcogen replacement, from O to Te, increases the amide rotation barrier somewhat, from 17.2 kcal mol^{-1} in formamide to 21.0 kcal mol^{-1} in telluroformamide. A similar increase was noted by Wiberg and Rablen[9] and Laidig and Cameron[10] in their studies of thioformamide. As the qualitative details of our

(13) (a) Foster, J. P.; Weinhold, F. *J. Am. Chem. Soc.* **1980**, *102*, 7211. (b) Reed, A. E.; Curtiss, L. A.; Weinhold, F. *Chem. Rev.* **1988**, *88*, 899.

(14) NPA: Reed, A. E.; Weinstock, R. B.; Weinhold, F. *J. Chem. Phys.* **1985**, *83*, 735. NPA is implemented in L607 (NBO 3.1) of the Gaussian program (ref 17).

(15) NRT: (a) Glendening, E. D. Ph.D. Thesis, University of Wisconsin, Madison, WI, 1991. (b) Glendening, E. D.; Weinhold, F. *J. Comput. Chem.*, submitted. NRT is implemented in version 4.0 of the NBO program (ref 16).

(16) (a) Glendening, E. D.; Badenhoop, J. K; Reed, A. E.; Carpenter, J. E.; Weinhold, F. *NBO 4.0*; Theoretical Chemistry Institute: Madison, WI, 1996. (b) Weinhold, F. *NBO 4.0 Program Manual*; Theoretical Chemistry Institute: Madison, WI, 1996.

(17) Frisch, M. J.; Trucks, G. W.; Schlegel, H. B.; Gill, P. M. W.; Johnson, B. G.; Robb, M. A.; Cheeseman, J. R.; Keith, T. A.; Petersson, G. A.; Montgomery, J. A.; Raghavachari, K.; Al-Laham, M. A.; Zakrzewski, V. G.; Ortiz, J. V.; Foresman, J. B.; Cioslowski, J.; Stefanov, B. B.; Nanayakkara, A.; Challacombe, M.; Peng, C. Y.; Ayala, P. Y.; Chen, W.; Wong, M. W.; Andres, J. L.; Replogle, E. S.; Gomperts, R.; Martin, R. L.; Fox, D. J.; Binkley, J. S.; Defrees, D. J.; Baker, J.; Stewart, J. P.; Head-Gordon, M.; Gonzalez, C.; Pople, J. A. *Gaussian 94, Rev C.3;* Gaussian, Inc.: Pittsburgh, PA, 1995.

(18) Schmidt, M. W.; Baldridge, K. K.; Boatz, J. A.; Elbert, S. T.; Gordon, M. S.; Jensen, J. H.; Koseki, S.; Matsunaga, N.; Nguyen, K. A.; Su, S.; Windus, T. L.; Dupuis, M.; Montgomery, J. A., Jr. *J. Comput. Chem.* **1993**, *14*, 1347.

(19) For a comprehensive review of the ab initio methods and all-electron basis sets employed in this work, see: Hehre, W. J.; Radom, L.; Schleyer, P. v. R.; Pople, J. A. *Ab Initio Molecular Orbital Theory*; Wiley: New York, 1986.

(20) B3LYP: (a) Becke, A. D. *J. Chem. Phys.* **1993**, *98*, 5648. (b) Lee, C.; Yang, W.; Parr, R. G. *Phys. Rev. B* **1988**, *37*, 785.

(21) Bergner, A.; Dolg, M.; Kuechle, W.; Stoll, H.; Preuss, H. *Mol. Phys.* **1993**, *80*, 1431.

Table 1. Optimized Structural Parameters and Rotation Barriers in the Amides $NH_2C(=X)H$

	planar (**1**)		twisted (**2**)		ΔE_{rot}
X	r_{CX} (Å)	r_{CN} (Å)	r_{CX} (Å)	r_{CN} (Å)	(kcal mol^{-1})
			RHF/6-31+G*		
O	1.195	1.348	1.184	1.426	16.1
S	1.641	1.325	1.605	1.423	21.0
Se	1.790	1.318	1.742	1.420	22.8
Te	2.027	1.309	1.957	1.420	26.9
			B3LYP/6-31+G*		
O	1.220	1.362	1.208	1.441	18.4
S	1.649	1.347	1.627	1.436	22.0
Se	1.793	1.342	1.766	1.431	22.7
Te	2.004	1.338	1.974	1.429	24.6
			MP2/6-31+G*		
O	1.230	1.362	1.221	1.441	17.2
S	1.636	1.352	1.621	1.438	19.5
Se	1.782	1.347	1.765	1.435	20.4
Te	1.992	1.344	1.972	1.435	21.0

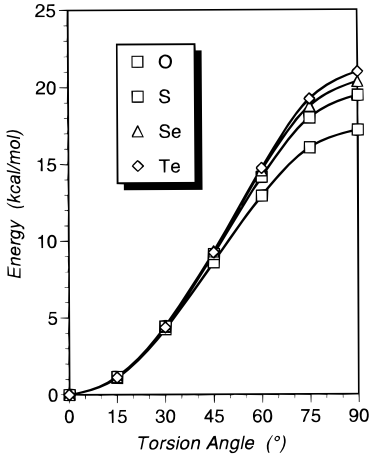

Figure 1. MP2 torsional profiles of formamide and its S, Se, and Te replacement analogues. The 0° and 90° rotamers correspond, respectively, to the geometries **1** and **2**.

calculations are essentially identical at the various levels of theory employed, we will primarily focus on the MP2 results.

Rotation strongly influences the amide geometries, particularly the CN bond length and, to a lesser degree, the CX bond length. The rotation of the planar geometries **1** into the twisted forms **2** is accompanied by a significant elongation of the CN bond. For example, the CN bond of formamide lengthens by 0.079 Å, from 1.362 Å in **1** to 1.441 Å in **2**. Similar, although somewhat larger, elongations are calculated for the CN bonds of the other amides (0.086, 0.088, and 0.091 Å for S, Se, and Te, respectively). At the same time, the CX bond contracts slightly (by 0.009, 0.015, 0.017, and 0.020 Å for O, S, Se, and Te, respectively). Clearly, the influence of rotation on bond length is more significant for the CN bond than for the CX.

As noted previously for formamide and thioformamide,[4−10] the disparity of these bond elongations/contractions conflicts somewhat with the resonance description of the amides. However, two electronic effects are involved in the amide rotations that can account, in part, for the differences. First, conjugative interactions involving the N lone pair and the CX π system can shorten or lengthen a bond by increasing or decreasing its double-bond character. This is the delocalizing effect treated by resonance theory. Second, a change of hybridization will tend to shorten or lengthen a bond as p-character is lost from or gained by its bonding hybrids. Conjugative interactions alone should influence the CX bond length as C and X are roughly sp^2 hybridized in both **1** and **2**.

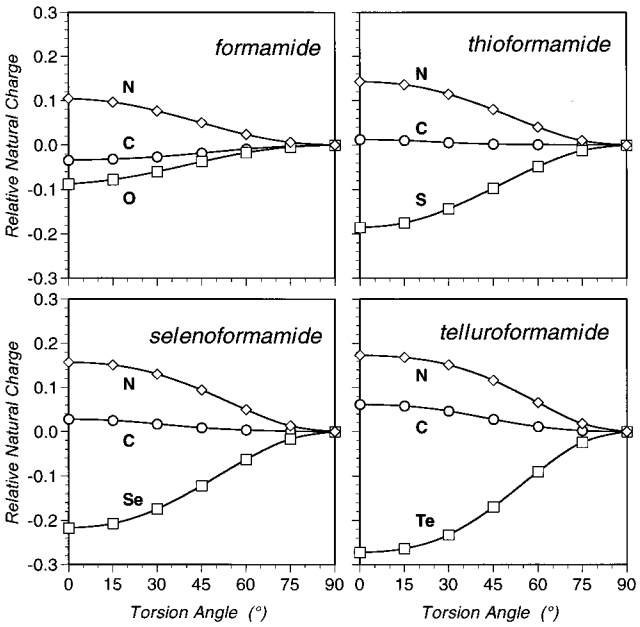

Figure 2. Torsional dependence of the MP2 natural charges of formamide and its S, Se, and Te replacement analogues. The charges are displayed relative to the absolute MP2 values of the twisted geometries **2** (the 90° rotamers).

But conjugation and hybridization both influence the CN bond length, the latter as N rehybridizes from sp^2 to sp^3 during the **1** → **2** rotation.

Constrained reoptimizations of the twisted amides were performed to determine the influence of rehybridization on CN bond length. Twisted geometries **4** were optimized in which

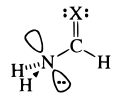

4

the amino group was constrained to have a locally planar configuration (hence, sp^2 hybridized N), while the N lone pair was rotated 90° out of conjugation with the CX π system. The difference between the optimized CN bond lengths of **4** and **2** reflects the influence of rehybridization alone as the N lone pair remains localized in both geometries. The MP2-optimized CN bond lengths of **4** (1.416, 1.410, 1.406, and 1.406 Å for O, S, Se, and Te, respectively) are 0.025−0.030 Å shorter than those of **2**. Thus, of the 0.079 Å contraction calculated for formamide, 0.025 Å results from the rehybridization of N while the remaining 0.054 Å arises from conjugative stabilization and other effects (*vide infra*). In general, roughly one-third of the elongation of the CN bond during the **1** → **2** rotation should be attributed to rehybridization.

IV. Population Analysis

Amide resonance suggests that the charge density of the planar geometry **1** should reflect the transfer of electron density from N to the chalcogen relative to that of the twisted geometry **2**. Whereas **2** is well represented by a single Lewis structure having no formal charges, **1** includes a significant contribution of the dipolar form **II** exhibiting formal positive and negative charges on the N and chalcogen centers, respectively. We consider here the influence of rotation (**2** → **1**) on the natural charges of NPA. Figure 2 shows the torsional dependence of the MP2 charges relative to the values calculated for the twisted geometries. The trends reflected in the RHF and B3LYP

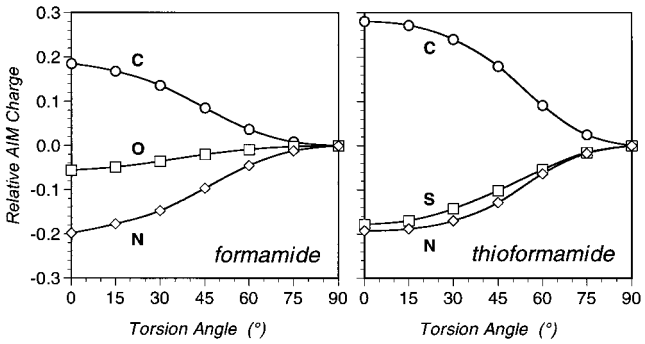

Figure 3. Similar to Figure 2, for the AIM charges.

charges are qualitatively identical to those at the MP2 level, so we only focus on the latter.[22]

The torsional dependence of the natural charges is largely consistent with the amide resonance model. Rotating the twisted geometries into the planar forms is principally accompanied by charge transfer from N to the chalcogen. For example, in formamide, N loses 0.105*e* while O gains 0.088*e*. The remaining charge density tends to collect at C (0.033*e*). Somewhat larger charge transfers are observed for the heavier chalcogens with greater involvement of the C atom. Thus, in telluroformamide, we find the transfer of 0.273*e* to Te, primarily from N (0.173*e*) and C (0.062*e*). Similar effects are calculated for the S and Se analogues.

It is perhaps surprising that charge transfer in the amides is stronger for the heavier chalcogens than for the lighter ones. Strong charge transfer implies a large contribution of the dipolar form **II**, which exhibits a formal negative charge on the chalcogen. The decreasing electronegativity of the chalcogens down the periodic table might lead one to anticipate diminished resonance stabilization and charge transfer. Nevertheless, the stronger charge transfer suggested by NPA is consistent with the increased rotation barriers and decreased CN bond lengths of the seleno- and telluroformamides. Clearly, it appears that the heavier chalcogens accommodate electron density more readily than expected on the basis of electronegativity. This property of the heavier chalcogens likely stems from their larger polarizabilities relative to the lighter atoms.[9,10]

In contrast to the natural charges, the AIM charges of Figure 3 reveal charge transfer that is largely inconsistent with the traditional amide resonance picture. The principal charge transfer during rotation (**2** → **1**) is from C to N.[9,10] Clearly, NPA and AIM give distinctly differing representations of the amide charge densities. What are we to conclude from this? Atomic charges cannot be uniquely defined, so neither NPA nor AIM should be considered to give the ''correct'' charges. We may inquire, however, which method yields the more appealing description of rotation in the amides. Here, it would seem that NPA is preferred as the natural charge shifts are essentially consistent with those anticipated from conventional resonance theory and chemical intuition. But perhaps the more compelling argument is that an orbital-based (Hilbert space) analysis like NPA supports the amide resonance model, an orbital-based description of electronic structure. AIM, a coordinate-based (real space) analysis, gives a largely contrasting view.

V. Natural Resonance Theory

NRT describes planar formamide (Table 2) as roughly a 2:1 mixture of two resonance structures, the parent Lewis structure **I** and secondary dipolar form **II**, respectively. At the RHF level, NRT calculates a set of 13 candidate structures, of which only the leading four are listed in Table 2. As expected, the structure of highest weight (65.40%) is the Lewis form **I**. NRT recognizes a strong $n_N \rightarrow \pi^*_{CO}$ interaction in the parent Lewis structure. This interaction is formally equivalent to the mixing of the dipolar form **II** (28.54%) in the resonance hybrid as it lends formamide CN double-bond character while tending to break the CO π bond. The Lewis and dipolar forms together account for 94% of the resonance hybrid. Two additional structures, **III** and **IV** (X = O) contribute about 2% each. These

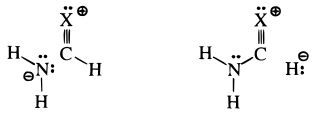

III **IV**

structures exhibit CO triple bonds and arise, respectively, from the delocalizing interactions of the in-plane p-type lone pair on O with the vicinal CN and CH antibonds ($n_O \rightarrow \sigma^*_{CN}$, $n_O \rightarrow \sigma^*_{CH}$). All other resonance forms have weights of less than 1%.

The B3LYP and MP2 level treatments of formamide yield a slightly more delocalized description of formamide. Electron correlation tends to weaken the contribution of the parent structure while increasing the weights of several of the secondary forms. Thus, we find that the Lewis and dipolar forms account for only 87% of the resonance hybrid at the MP2 level, down from 96% at RHF. Nevertheless, NRT's compact description of formamide remains qualitatively unchanged: formamide is principally a resonance hybrid of two contributing structures.

Natural bond orders reveal a significant exchange of bonding interaction in planar formamide, the CN bond gaining double-bond character at the expense of the carbonyl. At the RHF level, the CN bond (b_{CN} = 1.292) has roughly 29% double-bond character while the CO double bond has about 26% single-bond character (b_{CO} = 1.744). Electron correlation tends to increase the CN double-bond character. At the MP2 level, NRT calculates a CN bond order of 1.340, about 5% larger than the RHF value.

Table 2. Natural Resonance Weights and Bond Orders for Planar Formamide[a]

structure	interaction[b]	RHF	B3LYP	MP2
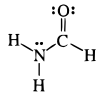		65.40	61.62	58.63
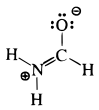	$n_N \rightarrow \pi^*_{CO}$	28.54	30.86	28.61
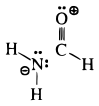	$n_O \rightarrow \sigma^*_{CN}$	1.95	2.35	3.10
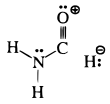	$n_O \rightarrow \sigma^*_{CH}$	1.93	2.31	2.05
others		2.22	2.86	7.61
	bond orders	RHF	B3LYP	MP2
	b_{CN}	1.292	1.320	1.340
	b_{CO}	1.744	1.725	1.717

[a] All geometries are optimized at the respective RHF, B3LYP, and MP2 levels of theory. Percentage weights are listed. [b] The orbital interaction of the parent Lewis structure that gives rise to the secondary forms.

(22) Natural charges for the planar and saddle point geometries of formamide and thioformamide were previously reported by Wiberg and Rablen (ref 9) at the MP2(full)/6-31+G* level but were not discussed in detail.

Table 3. MP2 Natural Resonance Weights and Bond Orders for Planar Formamide and its S, Se, and Te Replacement Analogues[a]

structure	X = O	X = S	X = Se	X = Te
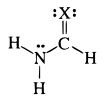	58.63	58.61	57.13	56.09
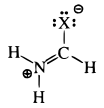	28.61	29.23	31.01	32.66
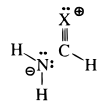	3.10	2.80	2.52	2.23
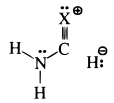	2.05	1.49	1.23	0.80
others	7.61	7.87	8.11	8.22
bond orders	X = O	X = S	X = Se	X = Te
b_{CN}	1.340	1.355	1.381	1.405
b_{CX}	1.717	1.694	1.664	1.636

[a] All geometries are optimized at the MP2 level. Percentage weights are listed.

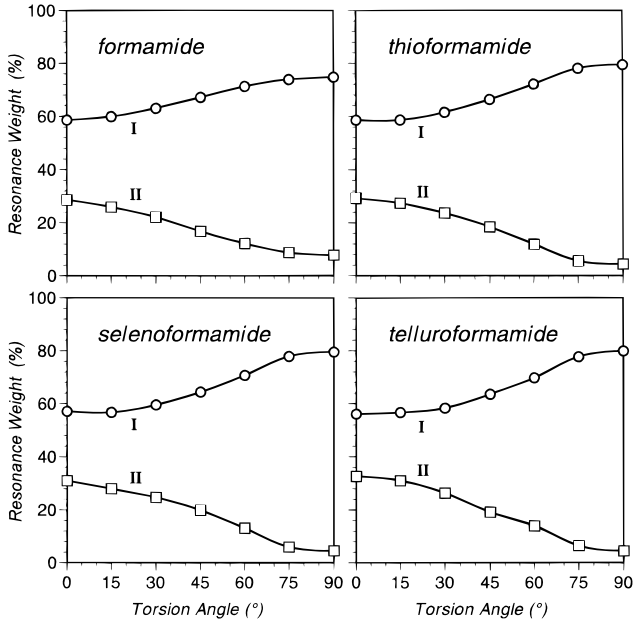

Figure 4. Torsional dependence of the MP2 natural weights of the Lewis (**I**) and dipolar (**II**) resonance structures for formamide and its S, Se, and Te replacement analogues.

Replacing the O of formamide by one of the heavier chalcogens strengthens the principal $n_N \rightarrow \pi^*_{CX}$ resonance interaction. Table 3 compares planar formamide with its chalcogen replacement analogues at the MP2 level. The weight of structure **II** increases from 28.61% in formamide to 29.23%, 31.01%, and 32.66% in the S, Se, and Te analogues, respectively. As a result, CN double-bond character increases from 34.0% in formamide to 40.5% in telluroformamide. These trends are fully consistent with the increasing rotation barriers and decreasing CN bond lengths discussed in section III and with the increasingly strong charge transfer from N to the chalcogen reflected by the natural charges of section IV.

Twisting the amides results in a considerable reduction in resonance stabilization. Figure 4 shows the torsional dependence of the MP2 weights for the Lewis (circles) and dipolar (squares) structures. There is a monotonic decrease in the

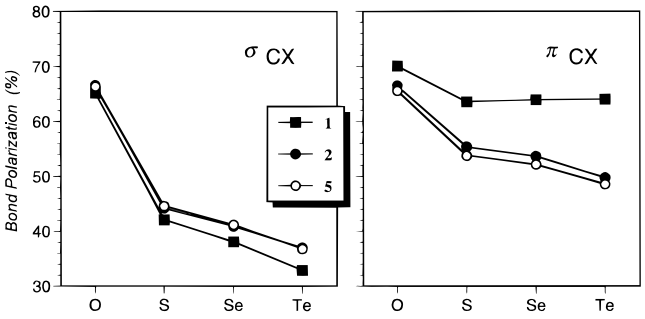

Figure 5. Torsional dependence of the MP2 polarizations of the σ_{CX} and π_{CX} bonds for formamide and thioformamide.

weight of the dipolar structure (and concomitant increase for the Lewis structure) as the amide is rotated from the planar into the twisted geometry. In formamide, the planar geometry has a 28.61% contribution from the dipolar form. This contribution decreases considerably to 7.79% in the twisted geometry as a strong π interaction ($n_N \rightarrow \pi^*_{CO}$) is exchanged for a substantially weaker σ one ($n_N \rightarrow \sigma^*_{CO}$).

A simple resonance treatment would suggest that the dipolar contribution **II** to the resonance hybrid should diminish with the decreasing electronegativity of the chalcogen.[9,10] In fact, the opposite trend is reflected by the NRT weights of Table 3. To determine the origin of this effect, we examined the character of the CX NBO of the parent Lewis structure and, in particular, how the polar covalent character of this orbital is influenced by the presence of a conjugating N lone pair. Bonding and antibonding NBOs $\{\sigma_{AB}, \sigma^*_{AB}\}$ are, respectively, in-phase and out-of-phase superpositions of two orthonormal atomic hybrids $\{h_A, h_B\}$

$$\sigma_{AB} = c_A h_A + c_B h_B \tag{5a}$$

$$\sigma^*_{AB} = c_B h_A - c_A h_B \tag{5b}$$

with coefficients $\{c_A, c_B\}$ chosen to maximize the occupancy of σ_{AB}. The polar covalence of these orbitals can be judged from the bond polarization (c_A^2). A bond polarization of 50% reflects a covalent bond, whereas polarizations of 100% and 0% describe fully ionic bonds, polarized completely toward atoms A and B, respectively. Figure 5 compares the polarizations of the σ_{CX} and π_{CX} NBOs of the planar and twisted amides (**1** and **2**) and aldehydes **5**,

5

where X = O, S, Se, and Te. The aldehydes are used to judge the nominal bond polarizations of the CX bonds in the absence of the amino group. The polarizations of Figure 5 are defined such that values larger than 50% correspond to bond polarization in the direction of the chalcogen.

The orientation of the N lone pair strongly influences the polarization of the π_{CX} bond, particularly for the heavier chalcogens. As shown in Figure 5, the π_{CX} bonds of **2** and **5**, which are not conjugated by an N lone pair, are essentially polarized to the same degree. Twisted formamide and formaldehyde, for example, have π_{CO} bonds that are 66.5% and 65.6% polarized toward O. Twisting the N lone pair into a conjugating position, as in **1**, tends to polarize further the π_{CX} bond toward the chalcogen (e.g., 70.1% in planar formamide). This effect is enhanced somewhat for the more polarizable chalcogens. Whereas the change in bond polarization in

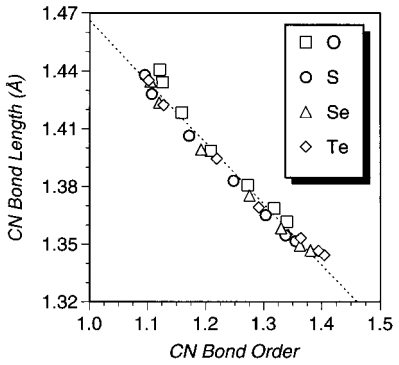

Figure 6. Approximate linear correlation of the MP2-optimized CN bond lengths with natural bond order for formamide and its S, Se, and Te replacement analogues.

formamide is about 5% (from 66.5% to 70.1%), the change in the Te analogue is nearly 15%, from 49.8% in twisted telluroformamide to 64.1% in the planar form. (The σ_{CX} bonds of **1**, **2**, and **5** are relatively insensitive to the presence or orientation of the N lone pair.) Polarizing the π_{CX} bond of **1** toward the chalcogen reverse polarizes the π^*_{CX} antibond toward C, making the latter a better acceptor for resonance interactions with the N lone pair ($n_N \rightarrow \pi^*_{CX}$). Thus, the higher polarizability of the heavier chalcogens facilitates repolarization of the π^*_{CX} antibond, leading to stronger resonance stabilization. Wiberg and Rablen[9] noted similar effects in a FMO analysis of formamide and thioformamide.

The lengthening of the CN bond as an amide is rotated from the planar to the twisted geometry is consistent with the loss of double-bond character reflected in the natural bond orders. Figure 6 shows the approximate linear relationship between the MP2-optimized CN bond lengths and natural bond orders for formamide and its chalcogen replacement analogues. For each of the amides, we show seven data points corresponding to the seven rotamer geometries optimized along the **1** → **2** torsional profile (cf. section III). Regression analysis gives a best fit line with a *y*-intercept of 1.467 Å (at $b_{CN} = 1$) and slope of −0.317 Å. The intercept is, in fact, essentially identical to the nominal single-bond length of methylamine (1.465 Å at MP2/6-31+G*), although the latter has an sp^3 hybridized C compared to the sp^2 hybridized one of **2**.

The CX bond lengths of the amides also exhibit an approximate linear correlation with natural bond order. Figure 7 shows the MP2-optimized CX bond lengths as a function of bond order for formamide and its S, Se, and Te analogues. Regression analysis of the data was performed using a linear expression of the form

$$R_{CX} = R_2 + m(b_{CX} - 2) \qquad (6)$$

where *m* is the CX bond length dependence on bond order and R_2 is the *y*-intercept at $b_{CX} = 2$ (the extrapolated, idealized double-bond length). Regression parameters are given in Table 4, together with the MP2-optimized CX bond lengths of the aldehydes **5**. The optimal R_2 values differ only marginally (by 0.009 Å or less) from the ideal CX double-bond lengths of the aldehydes.

The disparity between the slopes of Figures 6 and 7 is closely related to the differences in the CN and CX bond length variations discussed in section III. For example, whereas we find the CN bond length to contract 0.317 Å per unit bond order (Figure 6), the CO bond contracts only 0.047 Å (Figure 7 and Table 4). These values reflect the relatively large variation in CN bond length compared to the small variation for CO in formamide. As discussed in section III, a portion (perhaps one-

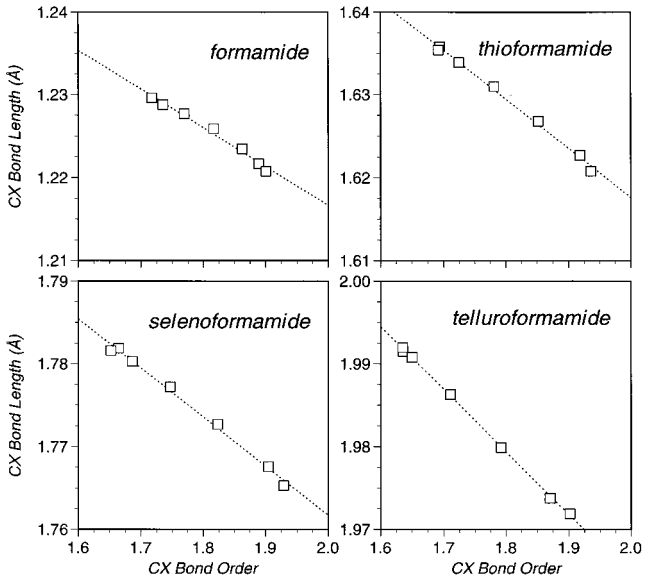

Figure 7. Similar to Figure 6, for the CX bond lengths of formamide and its S, Se, and Te replacement analogues. Regression parameters are given in Table 4.

Table 4. Regression Parameters of the MP2 CX Bond Length/Bond Order Correlation[a]

X	*m* (Å)	R_2 (Å)	R_{CX}[b] (Å)
O	−0.047	1.216	1.225
S	−0.059	1.618	1.619
Se	−0.059	1.762	1.760
Te	−0.076	1.963	1.961

[a] See text eq 7. [b] MP2-optimized CX bond lengths in formaldehyde, $H_2C{=}O$, and its S, Se, and Te replacement analogues.

third) of the difference arises from the rehybridization of N during rotation. There are, however, several additional factors that could contribute to the discrepancy. First, as shown in Figure 5, the π_{CX} bonds of the planar amides **1** are more ionic (polar) than those of the twisted forms **2**. The greater ionic character of CX in the planar geometries tends to strengthen and shorten these bonds despite the loss of double-bond character in **II**. Second, vibrational stretching frequencies suggest that double bonds are typically stiffer than single bonds. For example, the CO double bonds of amides have stretching frequencies near 1700 cm^{-1}, compared to 1180−1360 cm^{-1} for the CN single bonds of amines.[3] One might anticipate, therefore, that conjugation in the amides would more strongly influence the CN bond length than the CX bond. Third, the contributions of the triply-bonded structures **III** and **IV** may further stiffen the CX bonds. These structures account for roughly 5% of the resonance hybrid for planar formamide. Thus, through a combination of ionic and multiple bond character and rehybridization, it seems reasonable that the CN bond lengths of the amides are more strongly influenced by rotation than the CX bonds.

Finally, we find that the dipolar structure **II** is principally responsible for the planar configuration of the amino group. To determine the influence of this structure, we deleted its contribution from the resonance hybrid and reoptimized the planar amide geometry **1**. This was accomplished by zeroing the $n_N \rightarrow \pi^*_{CX}$ element of the NBO Fock matrix and constructing a ''localized'' wavefunction Ψ_{loc} from the resulting eigenvectors. Geometry optimization was then performed to minimize the energy of Ψ_{loc}. Details of these calculations are given in Table 5. The resonance energies *RE* (the energy differences between the ground state and localized amides in their respective optimized geometries) are a measure of the extra stability of

Table 5. Resonance Energies (*RE*) and Reoptimized Bond Lengths of the Localized Amides[a]

X	RE (kcal mol^{-1})	r_{CX} (Å)	r_{CN} (Å)
O	25.1	1.170	1.497
S	48.4	1.580	1.497
Se	51.4	1.712	1.498
Te	57.1	1.923	1.505

[a] RHF/6-31+G* values.

the planar amide geometries resulting from the dipolar contribution. As anticipated from our NRT results, *RE* increases monotonically down the periodic table, from 25.1 kcal mol^{-1} in formamide to 57.1 kcal mol^{-1} in telluroformamide.

These resonance energies are considerably larger than the corresponding rotation barriers (cf. Table 1). That is, the *localized* amides in the planar geometries **1** are less stable than the twisted geometries **2**. Indeed, vibrational frequencies analysis of the localized amides revealed that the planar geometries are unstable with respect to an out-of-plane distortion at N. Full geometry reoptimizations with no symmetry constraints allowed the localized amides to revert to the twisted geometries **2**. Thus, structure **II** (or alternatively the $n_N \rightarrow \pi^*_{CX}$ interaction) is responsible for the planar amide geometry. In the absence of its contribution, the amides would likely exhibit pyramidal geometries rather than planar ones.

VI. Summary

We have examined the rotation barriers of formamide and its S, Se, and Te replacement analogues using the NBO methods. NPA reveals the apparent transfer of electrons from N to the chalcogen in the planar, equilibrium amide geometries. NRT represents the planar amides as resonance hybrids consisting principally of two contributing structures, the parent Lewis form **I** and a secondary dipolar form **II**. In formamide, the sizable contribution of the dipolar form accounts for the planar amino geometry, large rotation barrier, and relatively short CN bond length. The weight of the dipolar form increases monotonically from formamide to telluroformamide in accord with the increasing rotation barrier and decreasing CN bond length. The larger polarizabilities of the heavier chalcogens allow these atoms to accommodate more charge density than anticipated on the basis of electronegativity. In short, the NBO methods reveal torsional behavior for formamide and its chalcogen replacement analogues that is largely consistent with the conventional amide resonance model.

Acknowledgment. This research was supported in part by a faculty startup grant from the Camille and Henry Dreyfus Foundation.

Supporting Information Available: A listing of the optimized amide geometries (in Gaussian 94 format) and raw energies (22 pages). See any current masthead page for ordering and Internet access instructions.

JA970074J